Available online at www.sciencedirect.com
ScienceDirect
Journal of Power Sources 173 (2007) 891–908
JOURNAL OF POWER SOURCES
www.elsevier.com/locate/jpowsour

Review

A review of heat-treatment effects on activity and stability of PEM fuel cell catalysts for oxygen reduction reaction

Cicero W.B. Bezerra [a,b], Lei Zhang [a], Hansan Liu [a], Kunchan Lee [a], Aldaléa L.B. Marques [c], Edmar P. Marques [b], Haijiang Wang [a], Jiujun Zhang [a,*]

[a] *Institute for Fuel Cell Innovation, National Research Council of Canada, Vancouver, BC V6T 1W5, Canada*
[b] *Department of Chemistry, Universidade Federal do Maranhão, Av. dos Portugueses, S/N 65.080-040 São Luís, MA, Brazil*
[c] *Department of Technology Chemistry, Universidade Federal do Maranhão, São Luís, MA, Brazil*

Received 25 June 2007; received in revised form 10 August 2007; accepted 13 August 2007
Available online 19 August 2007

Abstract

This paper reviews over 120 papers regarding the effect of heat treatment on the catalytic activity and stability of proton exchange membrane (PEM) fuel cell catalysts. These catalysts include primarily unsupported and carbon-supported platinum (Pt), Pt alloys, non-Pt alloys, and transition metal macrocycles. The heat treatment can induce changes in catalyst properties such as particle size, morphology, dispersion of the metal on the support, alloying degree, active site formation, catalytic activity, and catalytic stability. The optimum heat-treatment temperature and time period are strongly dependent on the individual catalyst. With respect to Pt-based catalysts, heat treatment can induce particle-size growth, better alloying degree, and changes in the catalyst surface morphology from amorphous to more ordered states, all of which have a remarkable effect on oxygen reduction reaction (ORR) activity and stability. However, heat treatment of the catalyst carbon supports can also significantly affect the ORR catalytic activity of the supported catalyst. Regarding non-noble catalysts, in particular transition metal macrocycles, heat treatment is also important in ORR activity and stability improvement. In fact, heat treatment is a necessary step for introducing more active catalytic sites. For metal chalcogenide catalysts, it seems that heat treatment may not be necessary for catalytic activity and stability improvement. More research is necessary to improve our fundamental understanding and to develop a new strategy that includes innovative heat-treatment processes for enhancing fuel cell catalyst activity and stability.
© 2007 Elsevier B.V. All rights reserved.

Keywords: Proton exchange membrane fuel cells; Electrocatalysis; Oxygen reduction reaction; Heat treatment; Pt catalysts; Non-noble catalysts

Contents

1. Introduction 892
2. Effects of heat treatment on carbon-supported Pt (Pt/C) catalysts 893
   2.1. Platinum particle size and morphology 893
   2.2. Carbon support 893
   2.3. Mechanism study 895
3. Effects of heat treatment on carbon-supported Pt alloy (Pt–M/C) and non-Pt–M/C catalysts 895
   3.1. Particle size and structural parameters 896
   3.2. Activity and stability 898
   3.3. Non-Pt–M/C catalysts 902
4. Effects of heat treatment on non-noble catalysts 902
   4.1. Transition metal macrocycles 902

* Corresponding author. Tel.: +1 604 221 3087.
E-mail address: jiujun.zhang@nrc.gc.ca (J. Zhang).

0378-7753/$ – see front matter © 2007 Elsevier B.V. All rights reserved.
doi:10.1016/j.jpowsour.2007.08.028

4.2. Transition metal chalcogenides 905
5. Conclusions 905
Acknowledgements 906
References 906

1. Introduction

Proton exchange membrane (PEM) fuel cells have been recognized as the most promising energy converting devices in terms of low or zero emissions and high efficiency [1–5]. It has been demonstrated that PEM fuel cells are able to meet transportation and stationary power requirements, which has driven further development of this technology towards commercialization. However, in this effort, two major technical gaps have been identified: high cost and low reliability and durability. The fuel cell catalyst is the major contributor to these difficulties. In recent years, although a great deal of effort has been put into the synthesis of cost-effective, active, and stable fuel cell catalysts, no real breakthroughs can be seen yet. Therefore, exploring breakthrough catalysts; improving catalyst activity, stability, and durability; and reducing catalyst cost are the major tasks in fuel cell commercialization [1–9].

At the current technical stage, the most practical catalysts in fuel cells are highly dispersed platinum (Pt)-based nanoparticles. These Pt nanoparticles are normally supported on carbon particles in order to increase the active Pt surface and improve the catalyst utilization. However, there are several drawbacks to Pt-based catalysts, such as high cost, sensitivity to contaminants, no tolerance to methanol oxidation (direct methanol fuel cell (DMFC) application), fewer completed four-electron reduction reactions, and Pt dissolution.

With respect to the exploration of alternative low-cost non-Pt catalysts, several other types of catalysts, including supported platinum group metal (PGM) such as Pd-, Ru- and Ir-based catalysts, bimetallic alloy catalysts, transition metal macrocycles, and transition metal chalcogenides, have been employed for PEM fuel cell catalysis [1,4,9]. The major force driving the development of non-Pt catalysts is a reduction in cost. However, these approaches are still in the research stage, as catalyst activity and stability are still too low to be practical when compared to Pt-based catalysts.

One of the major approaches to improving the activity and stability of Pt-based and non-Pt catalysts is to optimize the catalyst synthesis procedure. It is well known that the electrocatalyst performance is strongly dependent on the preparation procedures, including the addition of metal and its precursor, the support type and supporting strategy, and the heat-treatment strategy [10–16]. For example, even if the same catalyst with the same catalyst loading is used, the catalytic activity will differ depending on how the catalysts were attached to the electrode surfaces. Methods for catalyst attachment include irreversible adsorption, vacuum deposition, conducting polymer incorporation, porous carbon impregnation, and solvent evaporation [15].

Regarding ORR catalyst synthesis, heat-treatment has been recognized as an important and sometimes necessary step for catalytic activity improvement [16–21]. Many heat-treatment techniques, such as traditional oven/furnace heating [14,21], microwave heat-treatment [22–24], plasma thermal treatment [25–28], and ultrasonic spray pyrolysis [29], have been applied to prepare PEM fuel cell electrocatalysts. Among these, the traditional oven/furnace heating technique is the most widely used. In general, it involves heating the catalyst under an inert (N_2, Ar, or He) or reducing (H_2) atmosphere in the temperature range of 80–900 °C for 1–4 h [18,21].

For example, heat treatment or thermal activation for Pt-based catalyst synthesis has been considered a necessary step, which has a significant impact on the metal particle size and size distribution, particle surface morphology, and metal dispersion on the support [10]. The benefits of heat treatment are to remove any undesirable impurities resulting from early preparation stages, to allow a uniform dispersion and stable distribution of the metal on the support, and, therefore, to improve the electrocatalytic activity of the synthesized catalyst [18].

Another typical example is the heat treatment of macrocyclic metal complexes. Although the heat-treatment effect on these metal macrocycle properties has been well documented, a full understanding of the mechanism of catalytic activity improvement has not yet been achieved. When the catalysts are pyrolyzed at a desired high temperature in a flowing argon atmosphere, the molecular structure of the macrocycle is partially or completely destroyed, resulting in an catalyst with much better catalyst activity and stability than an untreated catalyst. Heat treatment can also affect the fundamental properties of the catalyst and its carbon support, including the loading level of the catalyst on the support, the number of catalytic sites, the acid–base properties of the support, and the distribution of the catalyst particles on the support.

The effect of heat treatment on catalyst properties is significant in terms of catalyst activity improvement. The mechanisms of the catalyst reaction during the heat-treatment process and the resulting improvement in activity are complicated and not fully understood. In addition, the relationship between heat treatment and the characteristics of the formed catalyst is also not completely clear. In order to accelerate the process of fuel cell catalyst development, a literature review would be of great benefit to the fuel cell catalyst community. In this paper, different catalyst heat-treatment strategies and their effects on the activities of several typical kinds of catalysts are reviewed, in order to summarize the current level of understanding of the catalyst improvement mechanisms caused by heat treatment.

2. Effects of heat treatment on carbon-supported Pt (Pt/C) catalysts

In PEM fuel cells including DMFCs, reactions include the oxygen reduction reaction (ORR) at the cathode and the H_2 (hydrogen fuel cells) or methanol (DMFCs) oxidation reaction (HOR or MOR) at the anode. In a hydrogen fuel cell, cathodic ORR is much slower than anodic HOR; therefore, the ORR is recognized as the determining reaction. In a DMFC, the rates of both ORR and MOR are slow and comparable. However, the slow ORR is still a problem in a DMFC. Therefore, the ORR catalysis will be our focus in this paper. It has been determined that the electrocatalytic reduction of molecular oxygen on a catalyst can be largely affected by catalyst particle size and surface structure [6,13,10,17,30–38]. Therefore, heat treatment can effectively change ORR activity and stability by altering the catalyst morphology.

2.1. Platinum particle size and morphology

With respect to the effect of Pt/C particle size on ORR activity, there seems to be no agreement in the literature. Several work reported that particle size had a significant effect on ORR activity, and that the optimum particle size was around 4 nm [32,36,39]. When Pt catalyst particle size was smaller than 3.5 nm, the catalyzed ORR rate was reduced. However, Yano et al. [37] recently investigated a series of carbon-supported Pt catalysts and found that the apparent ORR rate constant and the activation energies were independent of Pt particle size in the range of 1–5 nm. Bett et al. [40] also showed no dependency of Pt/C specific activity on the crystallite size in the range of 3–40 nm.

The literature suggests that catalytic ORR activity might be dependent on the relative concentrations of the Pt surface atoms, the coordination numbers of the localized atoms, and the ratio of preferable crystal planes on the crystallite surface [36,41]. However, Bett et al. [40] found that Pt atoms at the corners, edges, and kink sites or dislocation showed less ORR activity than those on the crystallite faces. Watanabe et al. [34] examined the influence of Pt crystallite size on ORR activity and found that the effect of crystallite dimensions was less important than that of the intercrystallite distances. They observed that when the crystallite distance was greater than approximately 18–20 nm, high-catalytic activity could be achieved, but if the Pt crystallites were too close, the specific activity of the catalyst was decreased.

For the heat-treatment effect on catalyst morphology, Han et al. [10] carried out conventional heat treatment of 20% Pt/C catalysts using several temperatures from 300 to 700 °C for various periods of time (3–9 h) in a nitrogen and hydrogen mixture atmosphere. The effect of heat treatment on CO oxidation was investigated using the cyclic voltammetry (CV) technique. They observed that the average particle sizes grew exponentially with the heating temperature and linearly with the heating time period. This observation was reported previously by Antolini [30] and Alexopoulos et al. [42], seperately.

Moreover, it also observed that the heat treatment could induce a uniform distribution of Pt over the support particles, resulting in well-defined cubo-octahedron crystallites, which were distinguishable from the initially irregular Pt surface [10]. As a result, the CO oxidation activity on this heat-treated Pt catalyst was improved significantly.

In addition, it was found that the CO oxidation activity was also dependent on the Pt particle size in the range of approximately 3–12 nm. The best catalytic performance was achieved for the catalyst with an average Pt particle size of about 5 nm.

The effect of heat treatment on the structural characteristics of the Pt/C catalyst was also observed by Antolini et al. [41]. Several Pt/C electrocatalysts were activated by dynamic heat treatment in an Ar atmosphere with two different heating rates of 15 and 45 °C min^{-1}. They observed that the heat treatment could lead to a growth in Pt particle size from 1 to 20 nm, independent of the nature of the carbon support. The catalysts treated at different heating rates showed the same variation of Pt particle size, but had different Pt crystallinities. The Pt crystallinity was decreased with an increasing heating rate. The heat treatment in the temperature range of 400–550 °C improved the Pt particle-size distribution on the support surface and showed the largest increase in Pt crystallinity.

In spite of some contradictory results on the effect of heat treatment on catalyst particle size, the effect on the ORR activity is clear; that is, heat treatment can effectively improve the ORR activity of a Pt/C electrocatalyst.

2.2. Carbon support

The catalyst support (i.e., carbon support) used in a fuel cell operation environment should be corrosion resistant and highly electrically conductive, and have a desirable water handling capability (hydrophilic character) [43,44]. Among all kinds of carbon supports (activated carbon, carbon black, graphite, and graphitized materials), carbon black is the most commonly used for electrocatalysis due to its high conductivity, excellent corrosion resistance, appropriate pore structure, and high-surface area [44–46]. Normally, graphitization is required in order to achieve a better level of corrosion resistance [45].

In practice, carbon supports are produced by burning carbonaceous materials. The properties of the carbon supports are strongly dependent on the nature of the starting materials and the preparation conditions, such as activation method, temperature, and heating time [43]. The surface of the formed carbon supports contains some oxygen functional groups, such as the carbonyl, carboxylic, phenolic, anhydride, lactonic and etheric groups. These functional groups can significantly affect the manufacture (loading and dispersion) and performance of the electrocatalysts, and are also responsible for both the acid–base and the redox properties of the carbon supports [5,16,45]. Generally, the surface oxygen-based groups can act as active or anchoring centers for the generation of highly dispersed catalyst metallic crystallites. The surface functional groups can also affect the catalyst deposition processes, including adsorption, ion-exchange or coordination, and deposition of metallic species by a redox reaction with specific groups on the carbon surface. For the adsorption process, the carbon support surface potential of zero charge seems to be of importance. It has been recognized that the

catalyst deposition process on the support is complicated. Mixed processes mentioned above could be involved in the catalyst deposition [44,45]. Several works [16,17,47–49] demonstrated that the number of oxygenated surface groups on the support could alter both the dispersion and the resistance of the sintered Pt/C catalysts.

For carbon-support heat treatment, Prado-Burguete et al. [47] prepared a series of Pt/C catalysts using different pre-heat-treated carbon supports. The effects of the pre-heat-treatment and chemical treatment on the carbon porous texture and amount of oxygen surface groups were investigated. In their experiments, carbon black samples were first heat treated at 950 °C in a H_2 flowing environment for 12 h. Two of the samples were then put into solutions containing 8 and 12N H_2O_2 for oxidation treatment. According to the N_2 adsorption isotherms for the supports, neither heat treatment in H_2 nor heat treatment followed by oxidizing treatment with peroxide changed the porous texture of the carbon support appreciably. However, further work [48] showed that heat treatment in a helium environment could produce a drastic change in the porous structure of the carbon support, resulting in a significant decrease in micro- and meso-porosity. Pt catalysts were prepared using those pre-treated supports at different temperatures and time periods. The results showed that H_2O_2 treatment could introduce new oxygen-containing surface species such as carboxylic and phenolic groups. With respect to the catalyst dispersion, the H_2O_2 oxidation-treated carbon support resulted in much better Pt dispersion than did the support that was only heat treated. This phenomenon was attributed to the large amount of oxygen-containing surface groups on the support. These groups can increase the wettability of the carbon particle surface, facilitating the metal precursor distribution throughout the particle surface at the impregnation and reduction steps of the catalyst synthesis. In addition, the catalyst formed on the H_2O_2 oxidation-treated support gave much better thermal stability.

Pre-graphitized carbon has also been used for the catalyst supports. Coloma et al. [16] studied three samples of pre-graphitized carbon blacks with the same porous texture. For comparison, different amounts of oxygen-containing surface groups were created by oxidation treatment with H_2O_2. They observed that the presence of these oxygen-containing groups affected the final dispersion of metallic Pt and the resistance to particle sintering, resulting in less favourable dispersion and lower sintering resistance. It was observed that at the impregnation step of the catalyst synthesis, the oxygenated groups on the support particles led to the best metal distribution. However, at the reduction step of Pt ions, the oxygen-containing groups were decomposed, causing a surface redistribution of the adsorbed Pt towards the π sites in the basal planes of the graphitic crystallites. Consequently, a less favourable Pt dispersion and a lower sintering resistance were produced.

Tian et al. [17] reported that heat treatment of the carbon support plays an important role in the improvement of Pt/C electrocatalytic activity towards ORR. Pt/C catalysts were prepared using heat-treated and untreated carbon black supports. Electrochemical performance of the Pt/C catalysts were evaluated based on the *current–voltage* curves of membrane electrode assembly (MEA) in a PEM fuel cell. The heat-treated supports were heated at 600 °C for 30 min in a N_2 environment. The results showed that the carbon surface composition, Pt particle size, and Pt dispersion were significantly affected by the heat treatment of the carbon support. The oxygen content in the heat-treated support sample was about 2.8 at.%, whereas that of the untreated one was 4.68 at.%. Transmission electron microscopy (TEM) and X-ray diffraction (XRD) for both the heat-treated and the untreated catalysts showed that the catalyst with the heat-treated support gave a smaller particle size and higher relative content of the Pt (1 1 1) crystal face. The average Pt particle sizes for the heat-treated and the untreated supports were 3.2 and 4.2 nm, respectively. Electrochemical measurement, using a Johnson Matthey Pt/C catalyst as the baseline, clearly indicated that the catalyst with a heat-treated support showed higher ORR activity than did the untreated one. In fact, its activity was similar to the baseline catalyst. Since the catalyst with the untreated support has a particle size close to that of the baseline catalyst, this result suggests that the particle size may not be a determining factor in electrocatalytic activity.

Antonucci et al. [13] prepared some carbon black-supported Pt electrocatalysts for the purpose of studying the interaction between Pt crystallites and the surface functional groups of the support. All catalysts studied were heat treated under reducing conditions in the temperature range of 400–900 °C. They showed that with an increase in the amount of oxygenated species on the carbon support, the Pt surface area was decreased. This may suggest that the Pt dispersion is sensitive to the heat treatment, which can produce different amounts of functional groups on the carbon surface depending on the heat-treatment temperature. It was also observed that with an increasing in the number of mildly acidic functionalities (pK_a was in the range 5.2–6.4), the metal dispersion improved; this result agreed with other observations [47,50]. Interestingly, a relationship between the metal surface area (MSA) and the number of basic functional groups of the support surface was also observed. Two distinct trends can be clearly seen in this relationship, depending on the roles of the different basic functionalities on the MSA. These two trends were believed to be associated with the different natures of the two basic groups: Cπ sites and pyrone-type complexes. In the former case, increasing the Cπ sites causes an increase in the Pt surface area, giving rise to higher metal dispersions and more electrochemically active sites. For pyrone-type groups, which have a strong basic property (produced at high-heat-treatment temperatures), can lead to the formation of Pt clusters, causing an increase in the particle size and a reduction in the number of electrochemically active Pt sites.

Torre et al. [50] carried out heat treatment on Pt/C catalysts prepared by three different methods in a flowing N_2 atmosphere at 200–900 °C for 45 min to approximately 4 h. Their main purpose was to study the effect of the acid–base properties of the carbon support on Pt dispersion. According to their results, heat-treatment increased the basic properties of the catalysts by removing acidic oxygen-containing groups from the particle surface to result in a greater number of Cπ sites and a pyrone-like structure [51]. Although the electrochemical activities of these catalysts were not evaluated, the active MSAs were determined

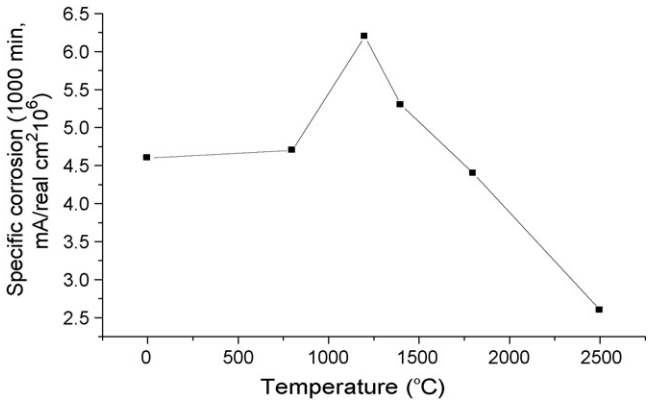

Fig. 1. Effect of heat-treatment on specific corrosion rate of Vulcan XC 72R. Corrosion currents recorded at 1.0 V in 180 °C H_3PO_4. [53].

in a H_3PO_4 solution using cyclic voltammetry. In addition, the Pt dispersion was also verified by TEM. Their results indicated that the metal surface areas decreased with the increasing temperature as well as with increasing pH_{ZPC}, i.e., a pH value where the surface exhibits a net zero charge. Their results suggested that 700 °C could be the optimum heat-treatment temperature in the weakly basic catalyst range.

Aricò et al. [51] evaluated the effect of Pt loading, heat treatment and air exposure on the acid–base properties of Pt/C catalysts. Heat treatment was performed in a dry N_2 flux, at the following temperatures and heating times: 110 °C, 4 h; 600 °C, 4 h; and 900 °C, 1 h. These authors also concluded that heat treatment causes changes in the catalyst surface by increasing the number of the basic sites.

It seems that the more oxygen-containing surface groups exist on the catalyst support surface, the worse the Pt distribution is. Heat treatment can change these surface groups from an acidic status to a basic one (an increase in Cπ functionalities), leading to a better distribution of Pt particles on the carbon support and consequently resulting in better catalyst ORR activity and stability, even in a fuel cell operation environment [13,14,17,39,41].

In addition, it was also observed that head treatment stabilized the carbon support against electrochemical corrosion [52,53]. Durability experiments conducted in a phosphoric acid fuel cell environment (1000 h at 191 °C) showed that the disordered portion of the carbon support was oxidized, whereas the outer crystalline shell remained intact [52]. Stonehart [53] showed that heat treatment could stabilize the carbon against corrosive degradation and increase the lifetime of fuel cell cathodes containing carbon support-based Pt catalysts, as shown in Fig. 1. The Pt catalysts with heat-treated carbon support were more stable than those with untreated supports due to the strong interaction between the Pt particles and the basic anchoring sites on the carbon surface. It was observed that heat treatment at 370 °C in air led to an improvement in the stability of this catalyst in a 60 °C sulphuric acid solution [30,52,54].

2.3. Mechanism study

With respect to the mechanism study, two effects induced by heat treatment should be considered: (1) changes in the surface functional groups of the support and (2) changes in Pt dispersion, morphology, and crystallite growth on the carbon support.

The carbon support surface is very heterogeneous and contains a wide variety of functional groups, which can significantly affect the chemical properties of such a surface. It has been widely recognized that the mostly common surface functional groups are those species containing oxygen, as mentioned above [5,16,40,55,56]. Thermal desorption of surface oxides, such as CO_2, CO, and H_2O, is the most common indicator of the surface oxygen-containing groups of carbon, which can be detected by a mass spectrometer and/or a gas chromatograph. The detected species evoluted at different temperatures can then be used to infer the carbon surface functional groups [55]. Fig. 2 shows that heat treatment can change carbon surface functional groups primarily by reducing the amount of oxygen-containing acidic species. As a result, the surface becomes more basic due to the increased number of π bonding formation (C=C) and the pyrone-like structure. However, heat treatment can also induce a graphitic structure through polymerization and aromatization of the nanocrystalline graphene [56]. In this graphitization process, high temperatures are necessary [6,16,45,56]. During the polymerization process, the polycyclic aromatic molecules are formed with the elimination of heteroatoms. At a temperature of approximately 1630 °C, the large aromatic molecules start to condense into graphene, and when the temperature is higher than about 1730 °C, aromatization occurs to form a graphitic structure. Polymerization and aromatization can be indicated by average lattice parameters extracted from XRS [56]. The temperature range in which graphitization occurs is between 827 and 2230 °C. Temperature can significantly affect the number and the quality of structural defects in the material [56]. Kijima et al. [57,58] investigated the reaction course of carbonization of poly(phenylenebutadiynylenes) (PPBs) in the temperature range of 200–600 °C. A mechanism was proposed for the formation of nano-carbonaceous layers.

Regarding Pt deposition on a carbon support, the decomposition and redistribution of surface oxygen-containing groups during heat treatment can affect the dispersion and growth of Pt crystallites [49]. Another recognized phenomenon is the thermal sintering of supported Pt even at relatively low temperatures [41]. This leads to the growth and then the crystallization of Pt particle size in the face-centered cubic structure. Several models have been proposed to explain the mechanisms of particle-size sintering and growth; the Smoluchowski and Ostwald ripening models are the most accepted ones [41,47]. In the first mechanism the metal transport on the support surface occurs through the migration of Pt crystallites and is followed by a coalescence of the particles. The second mechanism involves the evaporation of atoms from small crystallites and then condensation on larger ones in a process similar to the Ostwald ripening of dispersed precipitates in solution.

3. Effects of heat treatment on carbon-supported Pt alloy (Pt–M/C) and non-Pt–M/C catalysts

Pt alloys with various transition metals have been extensively studied in the effort to reduce catalyst cost and to improve

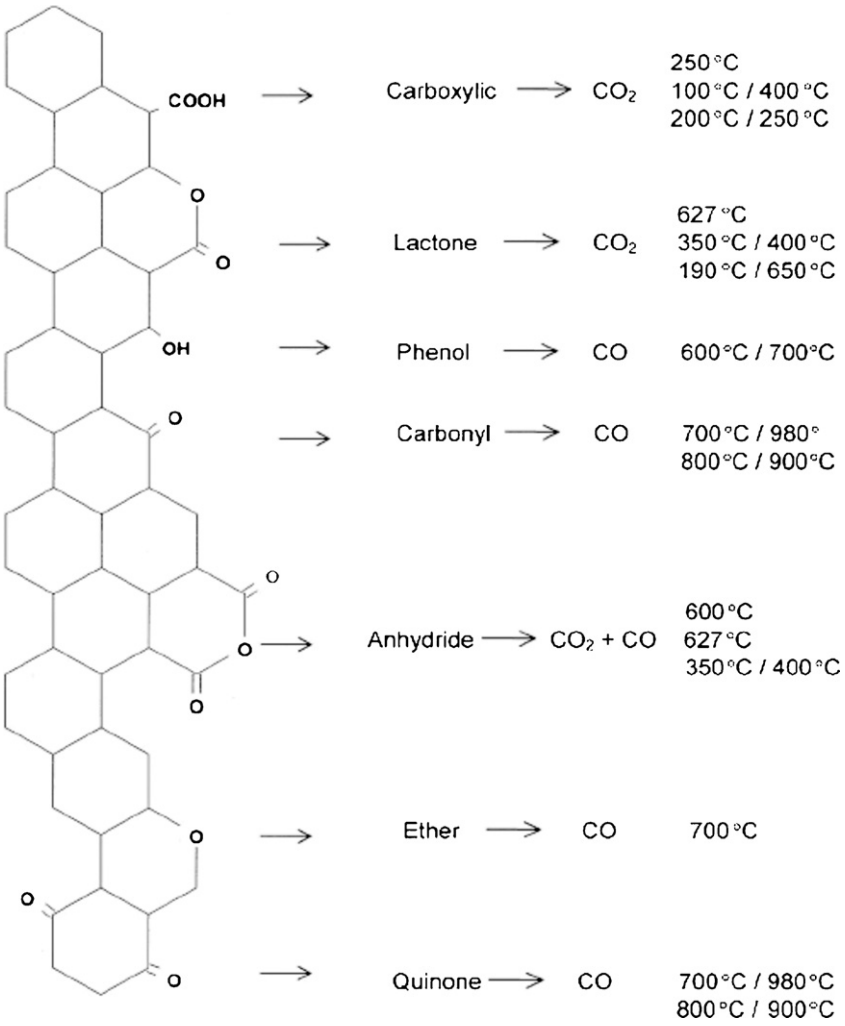

Fig. 2. Thermal decomposition products and corresponding evolution temperatures of carbon surface functional groups. Re-plotted from [55] by permission of The Electrochemical Society.

both the resistance to sintering and the electrocatalytic activity towards ORR [6,59,60]. There are many reports focusing on the synthesis and properties of Pt alloy catalysts mainly with V [61,62], Co [60,63–69], Fe [67,68], Ni [63,67,68] Cu [67,68,70], Ti [8,71], Pd [72] or Cr [73] as the second metal.

Generally, this kind of catalyst is prepared by deposition of the transition metal precursor on the Pt/C material, followed by chemical reduction and then alloying at high temperatures. The role of heat treatment is mainly to aid the formation of the alloy by increasing the mobility of the supported Pt. However, the high-temperature heat treatment can have a negative effect on the catalytic activity due to sintering and the growth of Pt particles. To avoid this, other procedures, such as simultaneous deposition and reduction of Pt and the second metal (M), the sol–gel process, and the polyol method, may be needed [59,64,69].

3.1. Particle size and structural parameters

Table 1 summarizes the literature data about the effect of heat treatment on particle size, lattice parameters, and alloying degree for carbon-supported Pt–M catalysts. A trend can be observed between the heat-treatment temperature and the particle size: with an increase in temperature, the particle size increases considerably due to the sintering of Pt particles.

The alloying of a second metal into the Pt can cause a change in the Pt lattice parameters, which can be directly observed by XRD. For example, a contraction in the lattice spacing or a shift in the position of the reflection peaks is indicative of the second metal being dissolved and of the formation of an ordered Pt–M phase. As seen in Table 1, when temperature is increased, the lattice constant decreases. According to Vegard's law, the lattice parameters are a linear function of the alloy composition if the temperature is fixed [73,74]. Thus, the degree of alloying can be determined by the value of these lattice parameters. It can also be seen in Table 1 that the degree of alloying formation is a function of the temperature. Therefore, heat-treatment temperature may be used to adjust the degree of the alloying.

It is not necessary for heat treatment to change the alloy properties of a catalyst. For example, when Cambanis and Chadwick [62] investigated a Pt–V alloy, not any evidence of intermetallic Pt_3V formation could be found even after heat treatment at temperatures ranging from 830 to 930 °C. However, Antolini et al.

Table 1
Effect of heat-treatment on structural parameters of reported Pt–M/C electrocatalysts

Second metal (M) in Pt–M/C (Pt:M)	Heat-treatment conditions	Treatment temperature/time period (T (°C)/t (h))	Particle size[a] (nm)	Lattice constant (Å)	Crystal structure	Alloying degree (%)	References
V (1:1)	As-prepared	–	3.4	3.8834	–	22	[61]
	Furnace (Ar/H_2)	500/2	3.9	3.8800	–	25	
		850/2	5.4	3.8686	fcc, Pt_2V	33	
Co (3:1)	Furnace (N_2/10% H_2)	600/2.5	3.83	3.855	fcc, Pt_3M		[63]
		700/2.5	2.95	3.876		61[b]	
		900/2.5	6.60	3.866		79[b]	
		1100/2.5	8.63	3.868		75[b]	
Cr (3:1)		700/2.5	4.23	3.903		39[b]	
		900/2.5	6.23	3.884		78[b]	
		1100/2.5	10.4	3.883		81[b]	
Ni (3:1)		700/2.5	4.62	3.858		53[b]	
		900/2.5	6.35	3.841		70[b]	
		1100/2.5	10.2	3.836		75[b]	
Co[c] (3:1)	As-prepared	–	3.4	3.925	–	–	[64]
	Furnace	700/2	8.4	3.870	fcc, Pt_3Co	–	
		900/2	8.0	3.867	–	–	
		1200/2	12.0	3.864	fcc, Pt_3Co	–	
Co[d] (3:1)	As-prepared	–	<2.5	3.927	–	–	
	Furnace	700/2	2.5	3.894	–	–	
		900/2	4.1	3.907	–	–	
		1200/2	10.4	3.910	–	–	
Co (3:1)	Furnace (H_2)	550/3	3.9	3.911		7	[66]
		900/3	6.8	3.897		35	
Co (3:1)	As-prepared	–	1.8	3.501		79	[69]
	Furnace (H_2)	400/2	9.6	3.90			
	Furnace (air/H_2)	200/1 (air) + 300/1 (H_2)	8.3	3.90			
Co (5:1)	As-prepared	–	3.6	–	–	–	[67]
	Furnace (Ar/10% H_2)	200/1	4.9	–	–	–	
		900/1	6.6	–	–	–	
Cu (3:1)	As-prepared	–	4.7	3.86	fcc, Pt_3Cu	–	[70]
	Furnace (Ar/10% H_2)	300/1	6.9	3.86		–	
		600/1	17.1	3.88		–	
		900/1	29.6	3.85		–	
Fe (1:1)	As-prepared	–	6.2	3.848(1)	Tetragonal	–	[68]
	Furnace (Ar/10% H_2)	500/1	6.3	3.847(1)		–	
		600/1	6.5	3.845(2)		–	
		800/1	6.8	3.848(1)		–	
Co (1:1)	As-prepared	–	5.5	3.782(1)		–	
	Furnace (Ar/10% H_2)	650/1	5.8	3.780(2)		–	
Ti[e]	As-prepared	–	4.8	3.926	–		[71]
	Furnace (He)	700/2	11.0	3.916	–		
		900/2	12.5	3.907	Pt_3Ti		
		1200/2	14.4	3.906	Pt_3Ti		
Ti[f]	As-prepared	–	<4.0	3.927	–		
	Furnace (He)	700/2	5.0	3.922	–		
		900/2	7.0	3.922	–		
		1200/2	28.0	3.908	Pt_3Ti		

Surface area measured by CO chemisorption.
[a] Measured by XRD.
[b] According to Ref. [59].
[c] Acidic route: $Co(OH)_2$ + HCl (pH 2).
[d] Alkaline route: $Co(NO_3)_2$ + NH_4OH (pH 11).
[e] Methanol:water solution (1:1).
[f] Methanol:water solution (1:1), pH 10.

[61] observed that the heat treatment of Pt–V/C at 850 °C led to the formation of an ordered phase (fcc Pt_2V).

The particle size and lattice constant of the alloy are also dependent on the preparation method. Heat-treated Pt–Co/C alloys prepared in acidic media (pH 2) showed larger particle sizes, more significant ordering, and greater alloying degree than those prepared in the basic media (pH 11) [64].

In the following section, the effect of the lattice structural parameters on the catalytic activity and stability of Pt–M/C catalysts will be discussed.

3.2. Activity and stability

The effects of electronic and geometric parameters such as Pt–Pt distance, metal particle size, and surface structure changes on the ORR catalytic activity and stability on the Pt/C catalysts discussed above are also applicable to the Pt–M/C catalysts. However, some differences between Pt/C and Pt–M/C should be emphasized [8,60,63,67–69,75–78].

For a Pt–M/C catalyst, the catalytic activity as well as the stability depends not only on the nature of Pt, but also on the second metal. In terms of ORR catalytic activity and tolerance to chemical corrosion, He et al. [8] classified the binary Pt–M alloy catalysts into four categories: (1) highly corrosive and highly active (M = Fe, Co, V, and Mn); (2) corrosive and highly active (M = Zn, Cu, Mo, and Ni); (3) stable, but less active (M = Zr, Cr, and Ta); and (4) stable and active (M = W and Ti).

A linear correlation between the ORR specific activity of Pt and Pt–M catalysts and Pt–Pt nearest neighbouring distance has been described in many works [61,65,76,79]. The smaller the Pt–Pt distance, the more active is the ORR catalytic activity. Heat treatment of an alloying catalyst at temperatures greater than 700 °C has two counteracting effects: (1) formation of a better Pt–M alloy, which decreases the Pt–Pt distance and affects the d-band vacancy of Pt, and thus improves the Pt electroactivity and (2) an increase in catalyst particle size, which decreases the active area of Pt, resulting in a depression of catalyst mass activity [62,80].

Some studies showed that the d-band vacancy strongly depends on the Pt particle size induced by heat-treatment [60,61,63]. According to current understanding, the hybridization of 5d state with empty states above the Fermi level can reduce the d-electron number. However, this hybridization will become less favourable once the particle size is increased.

With respect to a fundamental understanding of the ORR catalytic activity of alloys, Pd-based bimetallic catalysts, for example, were explored. A variety of hypotheses have been put forward to address the enhancement observed in comparison with a pure metal:

(1) Induced change in the density of states (DOS) at the Fermi level of Pd sites by alloy formation. Ota and co-worker's [81] considered that the decrease in DOS induced by electron transfer from the second element such as Co, Ni, or Cr to Pd may weaken the chemisorption bonds between Pd and reactants such as O_2, O/OH, O_2^-, and H_2O_2, reducing their respective blocking effect in the O_2 reduction process. As a result, ORR kinetics may be enhanced. For example, an alloyed Pd showed a reduced ORR overpotential by ~50 mV at 0.2 mA cm^{-2}, compared to that catalyzed by pure Pd.

(2) Induced change in the Gibbs free energy for the ORR. Wang and Balbuena [82] explained that if a catalyst consists of two metals, one with a low occupancy of d-orbitals (such as Co, Ni, Cr, or V) and the other with fully occupied d-orbitals (such as Pd, Au, and Ag), the d-orbital coupling effect between them can significantly decrease the Gibbs free energy for the electron transfer steps in the ORR, resulting in enhanced ORR kinetics.

(3) Pd lattice compression induced by alloy formation. A metal d-band center can be altered by orbital overlap. The formation of the alloy can induce Pd lattice compression (or reduction of bond lengths between metals), for example, via modification of electronic structures and orbital overlap. This will cause a shift of the d-band center, resulting in a change in the surface activity of the Pd sites. Density functional theory calculations made by Hammer and Norskov [83] confirmed that compression of the Pd lattice in Pd alloys could downshift the energy of the d-band center. Pd lattice compression can thus enhance the catalyzed ORR.

(4) Facilitated O_2 dissociation by alloy formation. Fernandez et al. [84] interpreted the enhancement in activity upon alloying using a simple thermodynamic model. They thought incorporation of more active metals into Pd, such as Co, could facilitate the dissociative adsorption of O_2 to form dissociated oxygen atoms (O_{ads}), and that these O_{ads} could migrate from the Co site to the Pd site whereupon electroreduction could occur with less polarization. For example, rotating disk electrode (RDE) experiments [84] showed a clear onset potential shift of ~200 mV in the positive direction for the ORR when Pd was alloyed with Co; and a Pd–Co alloy with an atomic ratio of 80:20 could give a optimum activity, which was very close to the activity exhibited by pure Pt catalysts.

(5) Formation of the desirable "Pd shell and alloy core" structure. Lu and co-worker's [85], in their recent paper on first-principles consideration in the design of Pd alloy catalysts for ORR, proposed that the key to improving the ORR activity of Pd-based catalysts is to alloy Pd with elements of smaller atomic size to form a "Pd shell and alloy core" structure, so as to take advantage of the lattice strain effect (lattice contraction induced by the incorporation of smaller atoms, such as Co, into the Pd lattice). This lattice strain effect can cause a downshift in the metal d-band center, weakening the interaction between the catalyst and the adsorbate (such as O_2). Three catalysts such as Pd, Pd–Co, and Pt showed experimentally an ORR activity order of Pt > Pd–Co > Pd, which is consistent with the theoretical interpretation [85].

The main stability-related problem of a Pt alloy catalyst is its dissolution in acid environments. However, the low stability of alloy catalysts is caused not only by the dissolution of the metal in the electrolyte, but also by the loss of active surface area partly due to the sintering [78,86].

Cambanis and Chadwick [62] prepared heat-treated Pt–V/C catalysts with different Pt/vanadium ratios. The heat treatment was performed at 830 and 930 °C. They observed that heat treatments at these two temperatures resulted in crystallite sizes in the ranges of 3.3–3.5 and 4.0–4.5 nm, respectively, independent of the vanadium content. These catalysts were tested for ORR at 180 °C in a phosphoric acid solution. It was found that the catalyst heat treated at 930 °C had less activity, which was attributed to the sintering effect. The results also showed that at both heat-treatment temperatures, the catalyst activities were dependent on the vanadium content, and the optimum vanadium content was in the range of 15–22 at.%.

Antolini et al. [61] heat-treated dispersed Pt–V alloy catalysts under a Ar + 10% H_2 atmosphere for 2 h at 500 and 850 °C in an effort to evaluate the effect of particle size and lattice parameters on the catalytic ORR performance in a PEM fuel cell. The catalyst treated at 850 °C showed a better ORR performance than did Pt/C due to the formation of an ordered phase (fcc Pt_2V) on the Pt–V alloy catalyst surface (fcc Pt_2V). XRD measurements indicated a decreased lattice parameter and an increased particle size (from 3.4 to 5.4 nm) with an increase in heat-treatment temperature (see Table 1). Heat treatment can increase the Pt–V alloy degree, resulting in enhanced catalytic activity towards ORR.

Min et al. [63] prepared three carbon-supported alloy catalysts (Pt–M/C, M = Co, Ni, Cr), and heat treated each of them separately at 600, 700, 900, and 1100 °C in a reducing atmosphere (N_2/10% H_2) for 2.5 h (Table 1). Their ORR catalytic activities were measured using a half-cell at an electrode potential of 900 mV (vs. dynamic hydrogen electrode). Measurements were carried out with pure oxygen in a 190 °C H_3PO_4 solution. The results showed that catalytic activity increased with increasing heat-treatment temperature, and the amount of increased activity was dependent on the nature of the second metal used in the alloying process, particle size and alloying degree with Pt. The altered Pt–Pt distance might be favourable for ORR.

Santiago et al. [69] prepared a carbon-supported $Pt_{70}Co_{30}$ nanoparticle catalyst using a polyol process. The catalyst had a very small particle size of 1.9 ± 0.2 nm. A carbon power was used for the support, which was heat treated at 850 °C for 5 h in an Ar atmosphere before the catalyst anchoring. The catalyst formed was heat treated again in different ways. The first sample was treated at 400 °C for 2 h in an H_2 atmosphere. The other sample was first treated at 200 °C for 1 h in air, followed by a 300 °C treatment for 1 h in an H_2 atmosphere. The ORR performance catalyzed by both as-prepared and heat-treated Pt–Co catalysts was better than that of commercially available Pt/C and Pt–Co (3:1)/C catalysts. In addition, both heat-treated samples showed an increase in the crystallite size compared to the as-prepared $Pt_{70}Co_{30}$/C (see Table 1). The electrocatalytic activities, measured by MEA testing, of the heat-treated and as-prepared samples were almost the same even though the as-prepared sample had a significantly smaller particles size than the heat-treated sample. Furthermore, the first sample heat-treated at 400 °C showed a significant performance loss in PEM fuel cell measurements. It is clear that the mutual functioning of the particle size, alloying, and surface oxides plays a role in catalyst activity improvement. More work is needed to distinguish which factor is dominant.

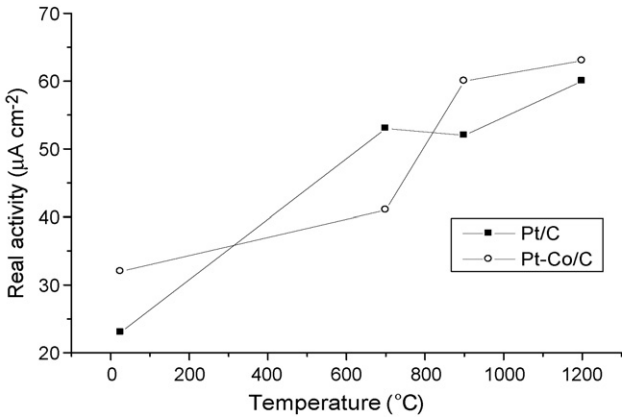

Fig. 3. Variation of the real activity of Pt/C and Pt–Co/C PAFC cathode catalysts as a function of heat-treatment temperature. Plotted according to the data in [64] by permission of The Electrochemical Society.

Beard and Ross [64] prepared Pt–Co/C alloys (3:1 atom ratio) using two methods: one in an acidic (pH 2) and the other in an alkaline (pH 11) aqueous medium. The synthesized catalysts were then heat treated at 700, 900, and 1200 °C, under an inert atmosphere for 2 h (for structural parameters, see Table 1). Fig. 3 shows the specific activity under phosphoric acid fuel cell conditions, of heat-treated Pt/C and Pt–Co/C catalysts (synthesized in acidic media) as a function of treatment temperature. It can be seen that heat treatment improves the catalyst activity in the whole temperature range, and that Pt–Co/C treated at 1200 °C shows a slightly higher specific activity than Pt/C. An important observation was the effect of the heat-treatment on Co loss. Untreated samples synthesized by both methods showed a Co loss of more than 80%, whereas the samples heat treated at 1200 °C showed losses of only 15% and 28.4% for acidic and alkaline routes, respectively. Therefore, heat treatment can effectively reduce Co loss.

Watanabe et al. [65] prepared Pt–Co/C catalysts and investigated the effect of heat treatment on their ORR catalytic activities and stability under the operating conditions of a phosphorous acid fuel cell. The heat treatment was performed in a reducing atmosphere (N_2 + 10% H_2) at several temperatures ranging from 400 to 900 °C for different time intervals under 20 h. They obtained well-defined alloys with ordered and disordered structures. The highest ordered structure was achieved with catalysts heat treated at temperatures between 600 and 650 °C for more than 5 h. A sample with disordered structure could be obtained by heating the ordered sample to 800 °C for 15 min, and then quenching it at a temperature lower than 400 °C. With the same heating time, the mean diameters of the Pt–Co alloy crystallites increased linearly with increasing heat-treatment temperature. Corrosion tests were performed by exposing these catalysts to a 210 °C H_3PO_4 solution for 0–50 h under a controlled potential of 0.8 V. It was found that Co atoms on the particle surfaces of both alloy catalysts dissolved easily in the acid media, but the disordered alloy was more corrosion resistant. The ORR performance of cathodes catalyzed by ordered and disordered catalyst

Table 2
Electrochemical characterization for Pt–Cu/C catalysts [70]

Pt–M/C (heat-treatment temperature, °C)	Electrochemical surface area ($cm^2\ mg^{-1}$)	At 700 mV (vs. Ag/AgCl)	
		Mass activity ($mA\ mg^{-1}$)	Specific activity ($mA\ cm^{-2}$)
Pt/C	679	332	0.49
Pt–Cu/C	423	323	0.76
Pt–Cu/C (300)	414	651	1.33
Pt–Cu/C (600)	333	217	0.65
Pt–Cu/C (900)	241	150	0.62

alloys in 50-h corrosion tests are shown in Fig. 4. It can be seen that before the corrosion test, the ordered catalyst exhibits a better specific activity (1.35 times higher than that of the disordered one). However, after the corrosion test, the ordered catalyst shows a decay in activity. It was concluded that the disordered alloy is preferable from the viewpoint of structure stability and electrocatalytic activity.

The effect of heat treatment on the structural and activity properties of Pt–Co/C alloy catalysts can also be seen from the work of Salgado et al. [66]. The catalysts were heat treated at 550 and 900 °C under a hydrogen atmosphere for 3 h (Table 1). Increases in particle size and contraction of the lattice were observed, suggesting a formation of better alloying with increasing temperature. Through ORR kinetic analysis in a single PEMFC fed with H_2/O_2, it was found that the sample treated at 550 °C was more active than that treated at 900 °C, although its alloying degree was poorer.

Tseng et al. [70] synthesized Pt–Cu/C alloy catalysts and studied the effects of precursor, preparation methods, and heat treatment on the catalyst particle size, dispersion, lattice structure, and ORR activity (Table 1). Due to the absence of two characteristic diffraction peaks in the XRD spectra, the authors speculated that all prepared catalysts were disordered phases with a face-centered cubic structure in which the Pt and Cu atoms were randomly distributed at the corner and face-centered positions. All Pt–Cu/C catalysts showed a smaller lattice constant and hence a shorter average Pt–Pt distance than did the pure Pt catalyst, and heat treatment had negligible effect on these parameters. Table 2 shows the catalyst surface areas and the ORR activities obtained by cyclic voltammetry for the catalysts before and after heat treatment. It can be clearly seen that the addition of copper caused a decrease in catalyst surface area. The catalyst heat treated at 300 °C gave the highest ORR activity. The authors concluded that the sample treated at 300 °C might favour O_2 adsorption and electron transfer on the Pt surface.

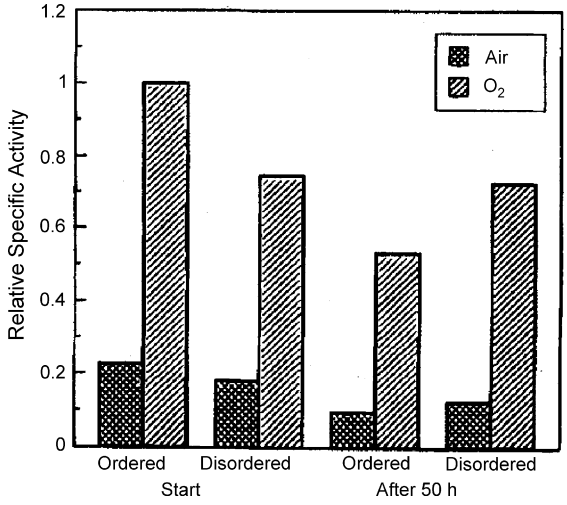

Fig. 4. The relative specific activities at 900 mV vs. RHE on the ordered and disordered alloy catalysts before and after the corrosion tests for 50 h at 0.8 V and at 210 °C in 105% H_3PO_4. Reproduced from [65] by permission of The Electrochemical Society.

Beard and Ross [71] prepared Pt–Ti/C catalysts in two solutions with different pHs. The as-prepared catalysts then were heat treated under a flowing He atmosphere for 2 h at 700, 900, and 1200 °C. Stability tests were carried out for 6 h in O_2-saturated 98% H_3PO_4 electrolyte (170 °C) and at a polarization potential range of 0.6–0.9 V (vs. reversible hydrogen electrode, RHE). It can be seen from Table 1 that with an increase in heat-treatment temperature, the particle size increases, resulting in an abrupt jump from 4.8 nm at room temperature to 11.0 nm at 700 °C for catalysts synthesized in the acidic route, and from 7.0 nm at 900 °C to 28.0 nm at 1200 °C for those prepared in the alkaline route. In addition, heat could created superlattice structures, suggesting the formation of the ordered alloy phase (Pt_3Ti). The stability test data for the catalysts prepared in the acidic route are summarized in Table 3. The results indicate significant losses of titanium, even in the heat-treated samples. Therefore, the titanium in the catalyst could not be stabilized by either alloying or heat treatment.

In an attempt to avoid alloy particle growth, Xiong et al. [67] prepared carbon-supported Pt–M alloys (M = Fe, Co, Ni and Cu) using a low-temperature (70 °C) method and investigated their ORR catalytic activity in a half-cell containing a sulphuric acid solution and in a PEM fuel cell cathode. Two alloy catalysts, Pt–Co/C and Pt–Fe/C, were separately heat-treated at 200 and 900 °C in an atmosphere of a flowing mixture of Ar + 10% H_2. They observed that the particle size increased with increas-

Table 3
Stability tests for Pt–Ti/C catalysts in phosphoric acid [71]

Pt–Ti/C (HT °C)	Pt/Ti ratio		Lattice constant (Å)	Superlattice
	Before	After		
As-prepared	42:1	57:1	3.927	No
700	–	–	3.928	No
900	–	–	3.910	Very weak
1200	29:1	48:1	3.907	Yes

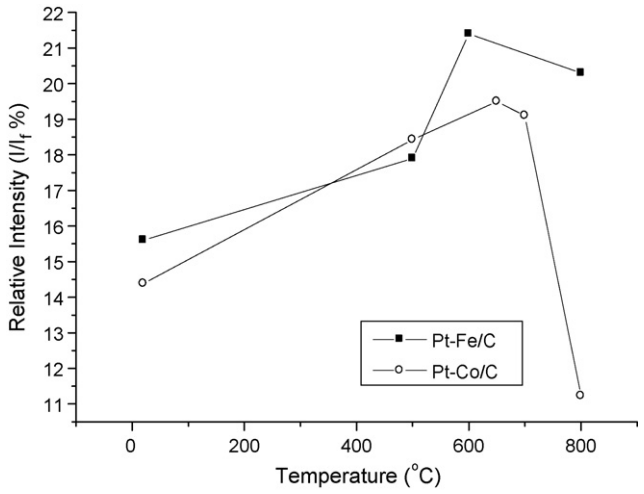

Fig. 5. Effect of the heating temperature on the extent of atomic ordering (I/I_f) for the Pt–Fe/C (I_{110}/I_{111}) and Pt–Co/C (I_{100}/I_{101}). Re-plotted from [68,87] by permission of The Royal Society of Chemistry and The Electrochemical Society.

ing heat-treatment temperature and time. The ORR activities of these two catalysts were improved by heat treatment at the lower temperature (200 °C). However, both catalysts treated at the higher temperature of 900 °C catalysts showed a dramatic degradation in ORR activity, which was attributed to the increase in particle size.

In a recent work, Xiong and Manthiram [68] synthesized several carbon-supported Pt–M alloys by first precipitating the M^{n+} hydroxide (M = Fe, Co, Ni or Cu) on commercially available Pt/C particles, and then heat treating them at 900 °C in a flowing mixture of Ar + 10% H_2. The ORR catalytic activities were validated in a PEM fuel cell. Pt–Fe/C and Pt–Co/C, contrary to other catalysts, showed ordered structures and enhanced ORR catalytic activity compared to Pt and disordered Pt alloys. The effect of heat-treatment temperature on the properties of Pt–Fe/C [68] and Pt–Co/C [87] was studied by heating these two catalysts at various temperatures from 500 to 900 °C for 1 h. The results are shown in Fig. 5. It can be seen that heat-treatment temperature of 600 and 650 °C produce the best ordering structure and consequently the highest catalytic activity.

Wei et al. [88] demonstrated that heat treatment plays a key role in obtaining a catalyst with proper corrosion resistance and a high-surface area. In their work, as-prepared Pt/C and Pt–Fe/C were heat treated separately at various temperatures from 95 to 900 °C in a flowing gas stream (N_2 + 7% H_2) for 40 min. Their results are shown in Table 4. It can be seen that the alloying degree and particle size are strongly dependent on the heat-treatment temperature. As usual, particle size increases with increasing the temperature. More interestingly, the Pt alloy catalysts exhibited a better resistance to sintering than did the pure Pt catalyst if the treatment temperature was higher. In addition, heat treatment could improve the stability of the catalysts in terms of dissolution reduction.

Roh et al. [86] prepared a carbon black-supported ternary Pt–Cu–Fe catalyst with a metal atomic ratio of 2:1:1. This as-prepared catalyst was then heat treated at 900 °C in a reducing atmosphere (N_2 + 10% H_2) for various periods from 0 to 5 h. The results indicated that when the heating time was increased, the ordered alloy extent increased accordingly, and the lattice structure of Pt changed from a face-centered cubic to a contracted face-centered tetragonal structure. After 2.5 h of heat treatment, the extent of the ordered alloy became larger. With respect to stability, these electrocatalysts were tested in a 200 °C H_3PO_4 (100%) medium under constant stirring in air for 5 h. It observed that more than 80% of both Cu and Fe in the non-heat-treated catalysts was dissolved during this test. In comparison, ordered alloys showed more stability than did the disordered ones. Regarding ORR performance in a fuel cell operation, ordered alloys produced by heat treatment showed improved catalytic activity compared to the pure Pt catalyst. The ORR activity of as-prepared catalyst alloys was lower than that of the baseline Pt/C catalyst, while heat-treated alloys showed slightly higher activity at the heat-treatment period of 2.5 h.

In summary, heat-treatment of as-prepared Pt–M/C catalysts increases the catalyst particle size, and at the same time, changes the catalyst lattice structure from a disordered one to a partially ordered one. It seems that the lattice structure change effectively improves the ORR catalytic activity and the catalyst stability, although the catalyst active area is reduced by the growth of particle size. Therefore, the negative effect of the catalyst particle size increase on the ORR activity may be overwhelmed by the positive effect of the lattice structure change.

Table 4
Effect of heat-treatment on stability and particle size of powder catalysts [88]

Catalyst	Heat-treatment temperature (°C)	Crystal detected by XRD	Dissolution of Pt after ageing[a] (%)	Metal particle size (nm)	
				Before ageing	After ageing
Pt/C	95	Pt	28.7	7.5	12.2
	750		2.1	35.8	36.3
	900		0.2	46.7	46.7
$Pt_{67}Fe_{33}$/C	500	–	11.4	23.4	30.1
	650	Pt, Pt_3Fe	10.4	20.6	21.4
	750	Pt_3Fe	9.2	13.5	12.7
	900		4.6	22.3	21.9

[a] 0.3 g immersed in 20 g 105% H_3PO_4, saturated with air at 204 °C, for 5 h and under open-circuit conditions.

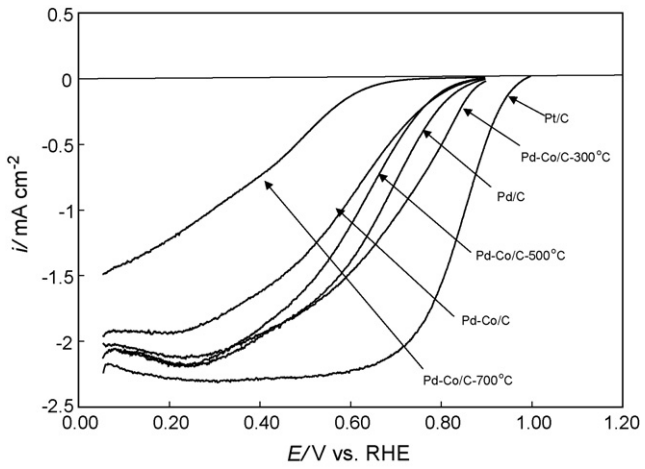

Fig. 6. Single scan voltammograms for Pt/C, Pd/C and Pd–Co/C alloys before and after heat-treatment at various temperatures in an oxygen saturated 0.5 M H_2SO_4 solutions at 25 °C. Potential scan rate: 5 mV s^{-1}. Reproduced from [90] by permission of Elsevier.

3.3. Non-Pt–M/C catalysts

Non-Pt alloy catalysts have been investigated for many years in an attempt to overcome the high cost and limited resources of Pt [89]. Typical examples are palladium (Pd)–M/C catalysts, which have the advantage of being methanol-tolerant ORR electrocatalysts [90–93].

The effect of heat treatment of Pd–M/C catalysts on the morphology and ORR activity were reported by several groups (M = Co [90,93]; Cu [94]; Fe [95]). Recently Zhang et al. [90] verified that heat-treatment is necessary to enhance the catalytic activity towards ORR of a carbon-supported Pd–Co alloy (Fig. 6). The maximum ORR activity was found when the sample was treated at 300 °C. However, different synthesis procedures can affect the catalyst properties. Zhang et al. [90] used an impregnation method and carried out heat-treatment with a temperature ramping rate of 5 °C min^{-1} under flowing N_2, at temperatures ranging from 300 to 700 °C for 2 h, while Wang et al. [93] prepared the same catalysts via a modified polyol reduction followed by a heat treatment for 2 h at 400–700 °C in an atmosphere of flowing N_2/10% H_2. Both works observed that with an increase in temperature, the catalyst lattice contraction, degree of alloying, and particles size were increased.

A similar effect on morphology and ORR electrocatalytic activity was observed when Cu [94] or Fe [95] was used as the second metal and the catalyst was heat treated in the temperature range of 300–800 °C. When the Pd:Cu ratio in Pd–Cu/C was 1:3, the best treatment temperature in terms of ORR activity improvement was 600 °C. For Pd–Fe/C, the best temperature was 500 °C.

4. Effects of heat treatment on non-noble catalysts

4.1. Transition metal macrocycles

Another kind of the fuel cell catalyst which has been extensively explored as a potential replacement for Pt for ORR catalysis is transition metal N_4-chelates (macrocycles). These promising cathodic catalysts have shown reasonable activity and remarkable selectivity towards ORR. They can catalyze a direct four-electron reduction of O_2 to produce water, and are inert to methanol oxidation [9,11,29]. However, practical catalysts in PEM fuel cells require strong activity and high stability, major barriers for this kind of catalyst.

It is generally recognized that the activity and stability of transition metal macrocycles for ORR catalysis could be significantly improved by heat treatment. In the past several decades, heat treatment has been employed to treat carbon-supported macrocyclic catalysts, and the attained catalysts showed considerable improvement in ORR stability and activity. However, long-term stability remains a problem. A possible cause might be the hydrogen peroxide produced in the ORR process, which could attack the catalyst and degrade its performance.

Jahnke et al. [96] showed that heat treatment had a significant effect on the ORR catalytic activity of carbon-supported CoTAA (dihydrodibenzotetraazaannulene). The results, shown in Fig. 7, indicate that all of the heat-treated CoTAA samples showed better ORR performance than did the untreated one. It seems that the best ORR activity was obtained at 600 °C, and the best stability was obtained at 800–900 °C. When heat-treatment temperature goes up over 1000 °C, both stability and activity are dropped sharply.

Among several other works dealing with CoTAA as an ORR electrocatalyst [97–101], Biloul et al. [98] tested the performance of cobalt (Co) porphyrins (cobalt tetramethoxyphenylporphyrin ($TpOCH_3PPCo$) and its derivative (CF_3PPCo)) and CoTAA as ORR electrocatalysts under fuel cell conditions. All of these macrocycles were vacuum-deposited on carbon black (Printex XE2) or on active charcoal (Norit SX ultra) to form supported catalysts. Then the resulting carbon-supported catalysts were heat treated at 500, 600 and 800 °C under an N_2 or Ar atmosphere for 2 h. The effects of supports, catalyst loadings, and heat-treatment temperatures on the ORR activity were investigated. According to polarization curves, if the treatment temperature was the same, the active charcoal-supported $TpOCH_3PPCo$ showed a better performance than did the carbon black-supported $TpOCH_3PPCo$. The optimal CoTAA loading

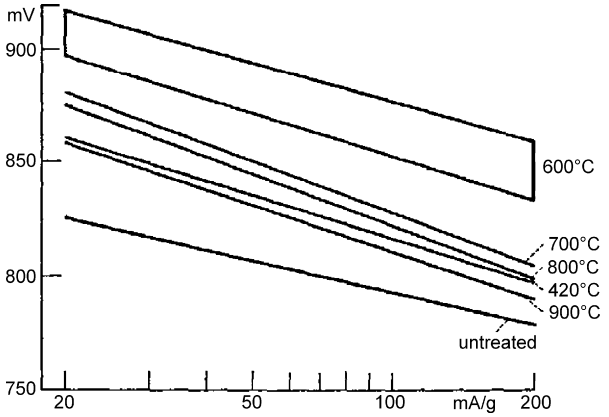

Fig. 7. Dependence of thermal activation on temperature (half-cell, electrolyte: 4.5N H_2SO_4). Reproduced from [96] by permission of Springer.

on the active charcoal support was found to be about 13 wt% at 800 °C. If other conditions such as catalyst type, loading, and support type were kept constant, the treated catalyst with the best ORR performance was the one treated at 800 °C. To discriminate the durability of different types of catalysts, a fuel cell with different cathode catalysts was tested at a current density of 100 mA cm^{-2} for less than 300 h. The observed durability order was $CF_3PPCo < TpOCH_3PPCo \ll CoTAA/SX$.

In an earlier work, Gouèrec et al. [102] observed that the optimal heat-treatment temperature of these carbon-supported tetraphenylporphyrins for ORR was 600 °C. Fig. 8 shows the electron spin resonance spectra of $TpOCH_3PPCo/SX$ and $TpCF_3PPCo/SX$ catalysts before and after the heat-treatment at 500, 600, and 800 °C. It can be seen that the untreated samples show the presence of Co porphyrins: $TpOCH_3PPCo(II)/TpOCH_3PPCo(III)O_2$ and $TPCF_3PPCo(II)$ (Fig. 8a and d, respectively). With an increase in heat-treatment temperature, the concentration of Co species in these samples decreases (Fig. 8b and e). Interestingly, even there is no visible Co present in the catalyst (800 °C-treated sample), ORR activity can also be observed.

Franke et al. [101] investigated the effect of heat treatment on the ORR catalytic activity of three transition metal macrocycles, CoTAA/C, FeTAA/C, and the metal-free H_2TAA/C. Heat treatment was performed in an inert atmosphere at different temperatures ranging from 150 to 1100 °C for different durations ranging from 0 to 8 h. When the heat-treatment time was short, the catalyst activities initially increased with the increase in heat-treatment temperature, and a peak activity was observed. Among all samples, the best active catalyst was CoTAA/C heat treated at a temperature of 600–700 °C. The metal-free catalyst showed visible activity only when the heat-treatment temperature was greater than 1000 °C.

The positive effect of heat treatment on the ORR stability and activity of CoTAA/C was also observed by Gouérec et al. [103]. The samples were heat treated under an N_2 or Ar atmosphere for 2 h at a temperature range of 500–900 °C. For the durability tests, the electrode modified by this heat-treated CoTAA/C was polarized at 500 mV (vs. RHE) for 100 h. It was found that the 600 °C samples showed the best performance in terms of activity and durability. The authors also showed that Co-involved bonding was different in these heat-treated catalysts. According to the results of X-ray photoelectron spectroscopy (XPS), the catalyst heat treated at 800 °C showed a complete demetallation. In order to discriminate the Co bonding in these materials, experiments with time-of-flight secondary ion mass spectrometry (ToF-SIMS) were carried out on unsupported catalysts (CoTAA and H_2TAA), carbon-supported catalysts (active charcoal-supported

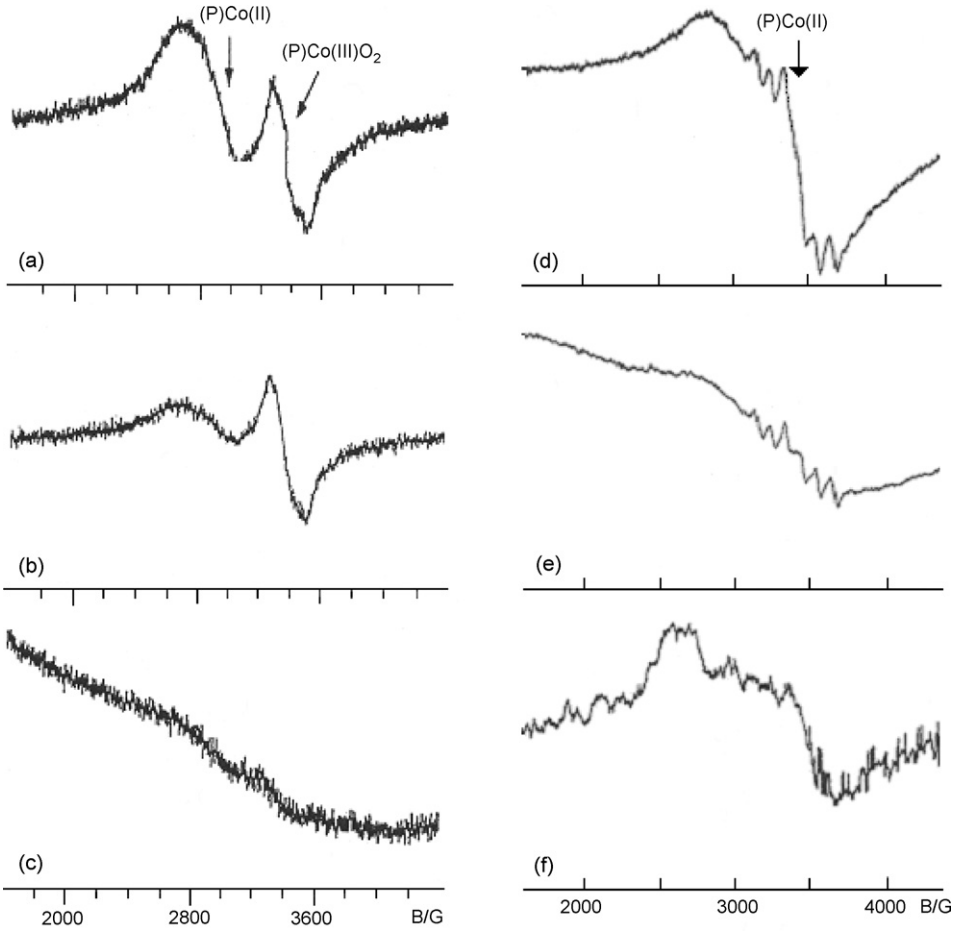

Fig. 8. ESR spectra of $TpOCH_3PPCo/SX$ Ultra on thermal treatment: (a) non-thermally treated; (b) 500 °C treated; (c) 800 °C treated, and $TpCF_3PPCo/SX$ (d) non-thermally treated; (e) 500 °C treated; (f) 800 °C treated. Reproduced from [102] by permission of Elsevier.

CoTAA (CoTAA/C) and H_2TAA (H_2TAA/C)), which were heat treated at different temperatures. On the positive side of the spectrum, pure CoTAA exhibited the parent ion ($C_{18}H_{14}N_4Co^+$) and its fragments such as Co^+, $C_8H_9N^+$, $C_9H_9N^+$, $C_7H_4NCo^+$, $C_{11}H_9N_2^+$, $C_7H_5N_2Co^+$, and $C_8H_4N_2Co^+$. On the negative side of the spectrum, several ions containing N and/or Co were detected, including CN^-, C_2N^-, C_3N^-, $C_2N_2Co^-$, $C_7H_5N_2^-$, and CN_4Co^-. However, after the CoTAA was deposited on the carbon, neither the parent ion nor the characteristic fragments could be seen on the positive side of the spectrum. On the negative side of the spectrum, only some fragments could be detected, including CN^-, C_2N^-, C_3N^-, CNO^-, and $C_2N_2Co^-$. The spectra of heat-treated and non-heat-treated CoTAA/C were similar, except the intensities of ions containing N and Co were decreased, and the intensities of Co and oxygen associated ions such as $CoOH^+$, CoO^-, $CoOH^-$, CoO_2^-, CoO_2H^-, and CoO_3^- were increased for heat-treated CoTAA/C. At 700 °C, for example, neither CoN_4 nor CoN_x were detected, suggesting a complete decomposition of the macrocycle. However, the intensity of the oxygenated Co fragments was significantly enhanced. Due to fact that the optimum ORR activity was found at 600 °C for the CoTAA/C catalyst, the detected fragments containing Co with N and/or O suggested that a stronger interaction between the metal in the CoN_x with oxygen surface groups on the support might play a role in catalyst activity enhancement. When the temperature went up to 800 °C, the macrocycle started to destruct, a favourable bonding of the nitrogen atoms, and the oxygen-containing group on the support surface appeared, resulting in a catalyst surface with a high content of Co oxide species.

Weng et al. [104] studied the carbon-supported Co phthalocyanine (CoPc) heat treated at different temperatures using ToF-SIMS coupled with XPS and TEM. The most active ORR CoPc/C catalyst was that heat treated at 600 °C under an inert atmosphere for 2 h [105], as illustrated in Fig. 9. Further studies [106,107] showed that the SIMS intensities of Co^+ and all other Co-containing organic fragments decreased with increasing heat-treatment temperature. The authors believed that the Co metal and/or the Co-containing fragments were responsible for catalytic activity enhancement in the temperature range of 600–700 °C.

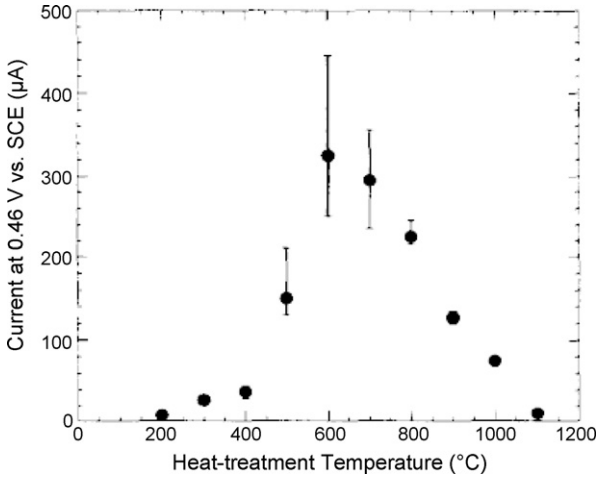

Fig. 9. Evolution of the catalyst electroactivity for the reduction of oxygen as a function of the heat-treatment temperature. Half-cell measurements, H_2SO_4 solution, pH 0.5. Reproduced from [104] by permission of Elsevier.

Since the structure of these N_4-chelate compounds could be partially or completely destroyed during pyrolysis at different heat-treatment temperatures, it can be expected that this type of electrocatalyst could be synthesized using common and inexpensive starting materials [1,9,108–111].

Lefèvre et al. prepared a series of Co-based [112] and Fe-based [108–110] ORR electrocatalysts by mixing the corresponding metal precursors. During the synthesis in a gas mixture of $NH_3 + H_2 + Ar$, the other experimental conditions, including ligands (acetate and porphyrin), metal loading (0.2% Co or Fe), and support (obtained by pyrolysis of perylene tetracarboxylic dianhydride (PTCDA)), were kept constant. The synthesized catalysts were then heat treated at the temperatures ranging from 400 to 1000 °C. It was observed that regardless of the precursor used, two catalytic sites for Fe-based catalysts were detected: FeN_4/C and FeN_2/C, which were represented by $FeN_4C_4^+$ and $FeN_2C_4^+$ ions, respectively. Their relative weights in the catalyst were dependent on the heat-treatment temperature. At temperatures above 700 °C, only FeN_2/C was more abundant, no matter which kind of Fe precursor was used. The correlation between the catalytic activity and the relative abundance of FeN_2/C at different heat-treatment temperatures suggested that the FeN_2/C site might be more active than the FeN_4/C site. In contrast to Fe-based catalysts, Co-based electrocatalysts had no dominant catalytic site such as $CoN_xC_y^+$. The best ORR catalytic activities for both types of catalysts were found to be at the heat-treatment temperature range of 500–800 °C.

A positive effect of heat-treatment on the ORR electrocatalytic activity of nanosized RuN_x catalysts was observed by Liu et al. [113]. This catalyst was supported on carbon particles using $RuCl_3$ and propylene diammine as the Ru and N precursors. The catalysts were then heat treated in an Ar atmosphere at a temperature range of 600–900 °C. As-prepared Ru-based chelate did not exhibit an ORR activity, suggesting that the active catalyst site was not formed. According to the authors' observation, a temperature of 700 °C gave the best ORR activity. As the temperature was increased beyond this point, the Ru crystallite size was gradually increased, forming catalyst agglomeration, which then negatively affected the catalyst activity.

In addition, some new heat-treatment techniques for synthesizing highly active macrocycle catalysts by creating favourable morphology and increasing surface area have been validated. Liu et al. [29] recently developed an ultrasonic spray pyrolysis (USP) technique to synthesize CoTMPP/C catalysts. This heat-method led to spherical, porous, and uniform CoTMPP/C particles with a high-surface area of 834 $m^2\ g^{-1}$. The ORR activity of the prepared catalyst was double that of the conventional heat-treated catalyst in an rotating ring-disk electrode (RRDE) measurement. As shown in Fig. 10, the results of H_2–air PEM single fuel cell testing showed that the cell performance of the USP-derived catalyst was much higher than that of the conventional heat-treated one.

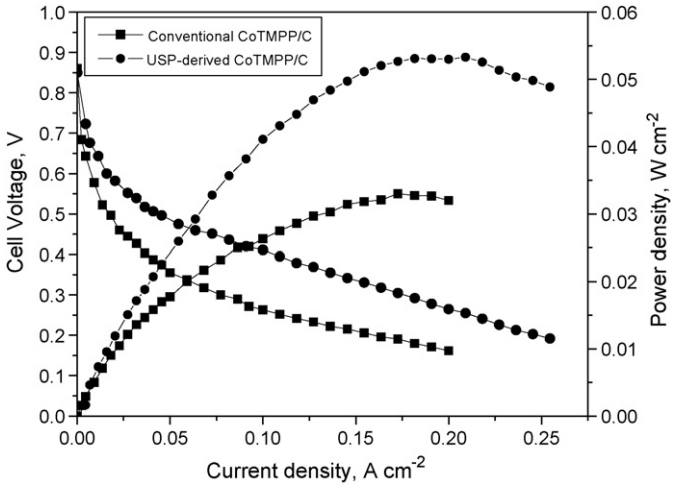

Fig. 10. Polarization and power density curves for H_2–air PEM fuel cells with conventional and ultrasonic spray pyrolysis (USP) derived CoTMPP/C catalysts. Reproduced from [29] by permission of Elsevier.

Bogdanoff et al. [25] developed another new heat-treatment technique, the plasma thermal treatment method, to suppress particle aggregation and increase surface area of macrocycle catalysts during the synthesis process. In this way, the electrochemical activity of the prepared catalysts was also effectively improved.

With respect to the applications of such transition metal macrocycle catalysts in cathode catalysis, although the ORR catalytic activity can be improved by with the assistance of techniques such as heat treatment, their stability in a fuel cell operation remains a challenge [11,96,98,103,110,113–117].

4.2. Transition metal chalcogenides

Transition metal chalcogenides, which have high-catalytic activity towards ORR and high-methanol tolerance [118–120], represent one type of non-Pt catalyst for fuel cell applications. Two typical chalcogenides are pseudo-binary selenides containing an Ru-substitute ($Mo_{6-x}Ru_xSe_8$, where $x = 1.8$ and 2.3) and ternary Ni-based tellurides ($Ni_{0.85}Mo_6Te_8$) [119]. The Ru-based compounds were prepared by sintering the mixtures of pure elements in a sealed quartz tube at high temperature (~1200 °C) for several hours. The Ni samples were prepared by reaction between binary Mo_6Te_8 and elemental Ni powder at 1000 °C [119–121]. It seems that there are few articles focusing on the effect of heat treatment on the ORR electrocatalytic properties of these materials. This is probably because the synthesis process is a high-temperature process and further heat-treatment may not be necessary [122].

However, some novel chalcogenide materials have been synthesized at low temperatures (<200 °C) by refluxing a metal carbonyl compound (such as $Mo(CO)_6$, $Ru_3(CO)_{12}$, $Os_3(CO)_{12}$) and the corresponding chalcogen. The temperatures used in the synthesis were limited by the boiling point of the organic solvent used. This faster, simple, and economic low-temperature procedure can produce cluster-like materials, which have improved electroactivity and chemical stability [122,123]. In most cases no further heat treatment is needed [1,124–126]. However, several works reported a subsequent stage of heat treatment [123,127,128]. For example, Reeve et al. [123] prepared carbon-supported $Mo_xRu_yS_z$, $Rh_xRu_yS_z$, and $Re_xRu_yS_z$ by refluxing the respective carbonyls with sulphur and carbon black in xylene for 20 h under nitrogen. The products were filtered, washed with acetone, dried, and finally heat treated at 350 °C for 2 h under nitrogen.

Regarding the effect of the heat-treatment on these catalysts, Rodríguez et al. [127] compared the ORR electrocatalytic activity of the as-prepared catalyst with the 500 °C heat-treated carbon-supported $Mo_xRu_ySe_z$ (predominant phase $Mo_4Ru_2Se_8$) catalysts. The as-prepared and heat-treated catalysts were all stable in acidic media, but the untreated sample exhibited much higher activity compared to the heat-treated one, which might be attributed to the loss of Se during the heat-treatment. Heat-treatment at over 250 °C for unsupported Ru-based catalysts could cause the release of carbon monoxide or carbon dioxide, resulting in a lower ORR catalytic activity [126].

Cheng et al. [128] observed that heat treatment under H_2 at 400 °C for 1 h improved the ORR catalytic activity and stability of an RuSe electrocatalyst. They observed that increasing the temperature beyond 400 °C would not lead to better performance. According to this study, the positive effect of heat treatment on the properties of such catalysts may be attributed to the following: (1) removal of the residual substances from the synthesis and emptying the pores, which may be utilized by new active sites formed from interactions between Ru, S, and C during heat treatment; (2) crystallisation that occurs during heat treatment, which causes a structural transition from an amorphous to a metallic state and reduces the electrical resistance; (3) reduction of the number of oxygen groups on the support surface, which enhances metal sintering. Such a reduction could decrease material sintering and, thus, increase the stability of these catalysts. As Ru can easily form Ru oxides in air, Se plays an important role in stabilizing the RuSe active site against further oxidation; and (4) formation of a catalytic site. As heat treatment has a significant effect on the catalyst composition, it has been assumed that the presence of new catalytic sites such as RuSe after heat-treatment can act as an electron reservoir and provide the adsorption sites for oxygen. The formation of such an active site is responsible for the higher activity and stability of the catalyst, although its real structure has to be identified.

5. Conclusions

Heat treatment of fuel cell catalysts plays an important role in the improvement of ORR electrocatalytic activity and stability. These catalysts primarily include unsupported and carbon-supported Pt, Pt alloys, non-Pt alloys, and transition metal macrocycles. The major effects of heat treatment on catalyst properties, including particle size, morphology, dispersion of the metal on the support, alloying degree, active site formation, catalytic activity, and catalytic stability, were reviewed in this paper. The optimum heat-treatment temperature and time period with respect to ORR activity and stability improvement are strongly dependent on the individual catalyst.

With respect to Pt-based catalysts, heat treatment can induce particle-size growth, better alloying degree, and changes in the catalyst surface morphology from amorphous to more ordered states, which have remarkable effects on ORR activity and stability. In addition, heat treatment of catalyst carbon supports can also affect the ORR catalytic activity of the supported catalyst significantly. However, if the heat-treatment temperature is too high (>1000 °C), even though the stability of the catalysts is improved, the catalytic activity could be degraded.

Heat treatment is also important for ORR activity and stability improvement of non-noble catalysts, in particular transition metal macrocycles. In fact, heat treatment is necessary for introducing more active catalytic sites. However, if the temperature is greater than about 800 °C, it could have a negative impact on the catalytic properties of these materials. For metal chalcogenide catalysts, it seems that heat treatment may not be necessary for catalytic activity and stability improvement.

The mechanisms of heat treatment, including induced catalyst surface structure change and surface active site formation, seem complicated. More fundamental research is necessary in order understand these mechanisms and to develop new strategies that include heat-treatment processes for enhancement in fuel cell catalyst activity and stability.

Acknowledgements

The authors thank the financial support of the Institute for Fuel Cell Innovation, National Research Council Canada (NRC-IFCI). Professor Cicero W.B. Bezerra (Grant holder from CNPq-Brazil) also wants to thank the financial support from Conselho Nacional de Desenvolvimento Científico e Tecnológico, Brazil (Proc. 202353/2006-0). The authors are also grateful to the CNPq (ETACOMB Proc. no. 505167/2004-2) and FINEP (DEFCCA Conv. no. 520186-2005-2) for financial support.

References

[1] L. Zhang, J. Zhang, D.P. Wilkson, H. Wang, J. Power Sources 156 (2006) 171–182.
[2] H. Liu, C. Song, L. Zhang, J. Zhang, H. Wang, D.P. Wilkinson, J. Power Sources 155 (2006) 95–110.
[3] K. Lee, J. Zhang, H. Wang, D.P. Wilkinson, J. Appl. Electrochem. 36 (2006) 507–522.
[4] R. Bashyam, P. Zelenay, Nature 443 (2006) 63–66.
[5] A. Guha, W. Lu, T.A. Zawodzinski, D.A. Schiraldi, Carbon 45 (2007) 1506–1517.
[6] S. Mukerjee, S. Srinivasan, in: W. Vielstich, A. Lamm, H.A. Gasteiger (Eds.), Handbook of Fuel Cells: Fundamentals, Technology and Applications. vol. 2. Electrocatalysis, Wiley, Chicester, 2003, pp. 502–519.
[7] M. Gattrell, B. MacDougall, in: W. Vielstich, A. Lamm, H.A. Gusteiger (Eds.), Handbook of Fuel Cells: Fundamentals, Technology and Applications. vol. 2. Electrocatalysis, Wiley, Chicester, 2003, pp. 443–464.
[8] T. He, E. Kreidler, L. Xiong, J. Luo, C.J. Zhong, J. Electrochem. Soc. 153 (2006) A1637–A1643.
[9] B. Wang, J. Power Sources 152 (2005) 1–15.
[10] K.S. Han, Y.S. Moon, O.H. Han, K.J. Hwang, I. Kim, H. Kim, Electrochem. Commun. 9 (2007) 317–324.
[11] P. Vasudevan, Santosh, M. Neelam, S. Tyagi, Transition Met. Chem. 15 (1990) 81–90.
[12] J. Luo, N. Kariuki, L. Han, L. Wang, C.J. Zhong, T. He, Electrochim. Acta 51 (2006) 4821–4827.
[13] P.L. Antonucci, V. Alderucci, N. Giordano, D.L. Cocke, H. Kim, J. Appl. Electrochem. 24 (1994) 58–65.
[14] S.J. Mukerjee, App. Electrochem. 20 (1990) 537–548.
[15] A. Elzing, A. van Der Putten, W. Visscher, E. Barendrecht, J. Electroanal. Chem. 200 (1986) 313–322.
[16] F. Coloma, A.S. Escribano, J.L.G. Fierro, F. Rodríguez-Reinoso, Langmuir 10 (1994) 750–755.
[17] J.H. Tian, F.B. Wang, Z.Q. Shan, R.J. Wang, J.Y. Zhang, J. Appl. Electrochem. 34 (2004) 461–467.
[18] G. Hinds, Preparation and characterisation of PEM fuel cell electrocatalysts: a review, NPL Report, United Kingdom, 2005, pp. 10–12.
[19] M. Kang, Y.S. Bae, C.H. Lee, Carbon 43 (2005) 1512–1516.
[20] M. Mazurek, N. Benker, C. Roth, H. Fuess, Fuel Cells 6 (2006) 208–213.
[21] H. Cheng, W. Yan, K. Scott, Fuel Cells 7 (2007) 16–20.
[22] R. Minami, Y. Kitamoto, T. Chikata, S. Kato, Electrochim. Acta 51 (2005) 864–866.
[23] M. Nie, P.K. Shen, M. Wu, Z. Wei, H. Meng, J. Power Sources 162 (2006) 173–176.
[24] Z.F. Ma, X.Y. Xie, X.X. Ma, D.Y. Zhang, Q. Ren, N. Heß-Mohr, V.M. Schmidt, Electrochem. Commun. 8 (2006) 389–394.
[25] P. Bogdanoff, I. Herrmann, M. Hilgendorff, I. Dorbandt, S. Fiechter, H. Tributsch, J. New Mater. Electrochem. Sys. 7 (2004) 85–92.
[26] I. Herrmann, V. Bruser, S. Fiechter, H. Kersten, P. Bogdanoff, J. Electrochem. Soc. 152 (2005) A2179–A2185.
[27] N.A. Savastenko, V. Brüser, M. Brüser, K. Anklam, S. Kutschera, H. Steffen, A. Schmuhl, J. Power Sources 165 (2007) 24–33.
[28] H. Shioyama, K. Honjo, M. Kiuchi, Y. Yamada, A.I. Ueda, N. Kuriyama, T. Kobayashi, J. Power Sources 161 (2006) 836–838.
[29] H. Liu, C. Song, Y. Tang, J. Zhang, J. Zhang, Electrochim. Acta 52 (2007) 4532–4538.
[30] E. Antolini, J. Mater. Sci. 38 (2003) 2995–3005.
[31] M.M. Shaijumon, S. Ramaprabhu, N. Rajalakshmi, Appl. Phys. Lett. 88 (2006) 253105.
[32] M. Peuckert, T. Yoneda, R.A.D. Betta, M. Boudart, J. Electrochem. Soc. 133 (1986) 944–947.
[33] Y. Takasy, N. Oshashi, X.G. Zhang, Y. Murakami, H. Minagawa, S. Sato, K. Yahikozawa, Electrochim. Acta 41 (1996) 2595–2600.
[34] M. Watanabe, H. Sei, P. Stonehart, J. Electroanal. Chem. 261 (1989) 375–387.
[35] T.J. Schmidt, V. Stamenkovic, M. Arenz, N.M. Markovic, P.N. Ross Jr., Electrochim. Acta 47 (2002) 3765–3776.
[36] K. Kinoshita, J. Electrochem. Soc. 137 (1990) 845–847.
[37] H.Y. Yano, J. Inukai, H. Uchida, M. Watanabe, P.K. Babu, T. Kobayashi, J.H. Chung, E. Oldfield, A. Wieckowski, Phys. Chem. Chem. Phys. 8 (2006) 4932–4939.
[38] A. Kabbabi, F. Gloaguen, F. Andolfatto, R. Durand, J. Electroanal. Chem. 373 (1994) 251–254.
[39] M.L. Sattler, P.N. Ross, Ultramicroscopy 20 (1986) 21–28.
[40] J. Bett, J. Lundquist, E. Washinton, P. Stonehart, Electrochim. Acta 18 (1973) 343–348.
[41] E. Antolini, F. Cardenilli, E. Giacomerri, G. Squadrito, J. Mater. Sci. 37 (2002) 133–139.
[42] A.H. Alexopoulos, A.I. Roussos, C.K. Kiparissides, Chem. Eng. Sci. 59 (2004) 5751–5769.
[43] D.S. Cameron, S.J. Cooper, I.L. Dodgson, B. Harrison, J.W. Jenkins, Catal. Today 7 (1990) 113–137.
[44] S. Kim, S.J. Park, Electrochim. Acta 52 (2007) 3013–3021.
[45] E. Auer, A. Freund, J. Pietsch, T. Tacke, Appl. Catal. A: Gen. 173 (1998) 259–271.
[46] G. Wang, G. Sun, Z. Zhou, J. Liu, Q. Wang, S. Wang, J. Guo, S. Yang, Q. Xin, B. Yi, Electrochem. Solid State Lett. 8 (2005) A12–A16.
[47] C. Prado-Burguete, A. Linares-Solano, F. Rodríguez-Reinoso, C.S.-M. Lecea, J. Catal. 115 (1989) 98–106.

[48] C. Prado-Burguete, A. Linares-Solano, F. Rodríguez-Reinoso, C.S.-M. Lecea, J. Catal. 128 (1991) 397–404.
[49] M.C. Roman-Martínez, D. Cazorla-Amorós, A. Linares-Solano, F. Rodríguez-Reinoso, C.S.-M. Lecea, H. Yamashita, M. Anpo, Carbon 33 (1995) 3–13.
[50] T. Torre, A.S. Aricó, V. Alderucci, V. Antonucci, N. Giordano, Appl. Catal. A: Gen. 114 (1994) 257–272.
[51] A.S. Aricò, V. Antonucci, L. Pino, P.L. Antonucci, N. Giordano, Carbon 28 (1990) 599–609.
[52] G.A. Gruver, J. Eletrochem. Soc. 125 (1978) 1719–1720.
[53] P. Stonehart, Carbon 22 (1984) 423–431.
[54] M. Uchida, Y. Aoyama, M. Tanabe, N. Yanagihara, N. Eda, A. Ohta, J. Electrochem. Soc. 142 (1995) 2572–2576.
[55] K.H. Kangasniemi, D.A. Condit, T.D. Jarvi, J. Electrochem. Soc. 151 (2004) E125–E132.
[56] R. Schlögl, in: G. Ertl, H. Knözinger, J. Weifkamp (Eds.), Handbook of Heterogeneous Catalysis, vol. 1, Wiley–VCH, Weinheim, 1997, pp. 138–191.
[57] M. Kijima, D. Fujiya, T. Oda, M. Ito, J. Therm. Anal. Calorim. 81 (2005) 549–554.
[58] M. Kijima, H. Tanimoto, K. Takakura, D. Fujiya, Y. Ayuta, K. Matsuishi, Carbon 45 (2007) 594–601.
[59] E. Antolini, Mater. Chem. Phys. 78 (2003) 563–573.
[60] E. Antolini, J.R.C. Salgado, M.J. Giz, E.R. Gonzalez, Int. J. Hydrogen Energy 30 (2005) 1213–1220.
[61] E. Antolini, R.R. Passos, E.A. Ticianelli, Electrochim. Acta 48 (2002) 263–270.
[62] G. Cambanis, D. Chadwick, Appl. Catal. 25 (1986) 191–198.
[63] M. Min, J. Cho, K. Cho, H. Kim, Electrochim. Acta 45 (2000) 4211–4217.
[64] B.C. Beard, P.N. Ross Jr., J. Electrochem. Soc. 137 (1990) 3368–3374.
[65] M. Watanabe, K. Tsurumi, T. Nakamura, P. Stonehart, J. Electrochem. Soc. 141 (1994) 2659–2668.
[66] J.R.C. Salgado, E. Antolini, E.R. Gonzalez, J. Phys. Chem. B 108 (2004) 17767–17774.
[67] L. Xiong, A.M. Kannan, A. Manthiram, Electrochem. Commun. 4 (2002) 898–903.
[68] L. Xiong, A. Manthiram, J. Electrochem. Soc. 152 (2005) A697–A703.
[69] E.I. Santiago, L.C. Varanda, H.M. Villullas, J. Phys. Chem. C 111 (2007) 3146–3151.
[70] C.J. Tseng, S.T. Lo, S.C. Lo, P.P. Chu, Mater. Chem. Phys. 100 (2006) 385–390.
[71] B.C. Beard, P.N. Ross Jr., J. Eletrochem. Soc. 133 (1986) 1839–1845.
[72] H. Li, G. Sun, N. Li, S. Sun, D. Su, Q. Xin, J. Phys. Chem. C 111 (2007) 5605–5617.
[73] J. Liu, M.M. Maye, V. Petkov, N.N. Kariuki, L. Wang, P. Njoki, D. Mott, Y. Lin, C.J. Zhong, Chem. Mater. 17 (2005) 3086–3091.
[74] A.R. Denton, N.W. Ashcroft, Phys. Rev. A 43 (1991) 3161–3164.
[75] E. Antolini, J.R.C. Salgado, E.R. Gonzalez, J. Power Sources 160 (2006) 957–968.
[76] V. Jalan, E.J. Taylor, J. Electrochem. Soc. 130 (1983) 2299–2302.
[77] S. Mukerjee, S. Srinivasan, M.P. Soriaga, J. McBreen, J. Electrochem. Soc. 142 (1995) 1409–1422.
[78] H.R. Colón-Mercado, B.N. Popov, J. Power Sources 155 (2006) 253–263.
[79] M.T. Paffett, J.G. Beery, S. Gottesfeld, J. Electrochem. Soc. 135 (1988) 1431–1436.
[80] H. Yang, W. Vogel, C. Lamy, N.C. Alonso-Vante, J. Phys. Chem. B 108 (2004) 11024–11034.
[81] K. Lee, O. Savadogo, A. Ishihara, S. Mitsushima, N. Kamiya, K.-I. Ota, J. Electrochem. Soc. 153 (1) (2006) A20–A24.
[82] Y. Wang, P.B. Balbuena, J. Phys. Chem. B 109 (2005) 18902–18906.
[83] B. Hammer, J.K. Norskov, Adv. Catal. 45 (2000) 71–129.
[84] J.L. Fernandez, D.A. Walsh, A.J. Bard, J. Am. Chem. Soc. 127 (2005) 357–365.
[85] Y. Suo, L. Zhuang, J. Lu, Angew. Chem. Int. Ed. 46 (2007) 2862–2864.
[86] W. Roh, J. Cho, H. Kim, J. Appl. Electrochem. 26 (1996) 623–630.
[87] L. Xiong, A. Manthiram, J. Mater. Chem. 14 (2004) 1454–1460.
[88] Z. Wei, H. Guo, Z. Tang, J. Power Sources 62 (1996) 233–236.
[89] V. Raghuveer, P.J. Ferreira, A. Manthiram, Electrochem. Commun. 8 (2006) 807–814.
[90] L. Zhang, K. Lee, J. Zhang, Electrochim. Acta 52 (2007) 3088–3094.
[91] J.L. Fernandez, V. Raghuveer, A. Manthiram, A.J. Bard, J. Am. Chem. Soc. 127 (2005) 13100–13101.
[92] V. Raghuveer, A. Manthiram, A.J. Bard, J. Phys. Chem. B 109 (2005) 22909–22912.
[93] W. Wang, D. Zheng, C. Du, Z. Zou, X. Zhang, B. Xia, H. Yang, D.L. Akins, J. Power Sources 167 (2007) 243–249.
[94] D. Myers, Proceedings of DOE Hydrogen Program Review, Arlington, VA, 2007.
[95] M.H. Shao, K. Sasaki, R.R. Adzic, J. Am. Chem. Soc. 128 (2006) 3526–3527.
[96] H. Jahnke, M. Schönborn, G. Zimmermann, Top. Curr. Chem. 61 (1976) 133–181.
[97] K. Wiesener, G. Grünig, J. Electroanal. Chem. 180 (1984) 639–643.
[98] A. Biloul, P. Gouèrec, M. Savy, G. Scarbeck, S. Besse, J. Riga, J. Appl. Electrochem. 26 (1996) 1139–1146.
[99] A. van Der Putten, A. Elzing, W. Visseher, E. Barendrecht, J. Electroanal. Chem. 205 (1986) 233–244.
[100] A. van Der Putten, A. Elzing, W. Visseher, E. Barendrecht, J. Electroanal. Chem. 221 (1987) 95–104.
[101] R. Franke, D. Ohms, K. Wiesener, J. Electroanal. Chem. 260 (1989) 63–73.
[102] P. Gouèrec, A. Biloul, O. Contamin, G. Scarbeck, M. Savy, J.M. Barbe, R. Guilard, J. Electroanal. Chem. 398 (1995) 67–75.
[103] P. Gouèrec, A. Biloul, O. Contamin, G. Scarbeck, M. Savy, J. Riga, L.T. Weng, P. Bertand, J. Electroanal. Chem. 422 (1997) 61–75.
[104] L.T. Weng, P. Bertrand, G. Lalande, D. Guay, J.P. Dodelet, Appl. Surf. Sci. 84 (1995) 9–21.
[105] G. Tamizhamani, J.P. Dodelet, D. Guay, G. Laland, G.A. Capuano, J. Electrochem. Soc. 141 (1994) 41–45.
[106] M. Ladouceur, G. Lalande, G. Guay, J.P. Dodelet, L. Dignard-Bailey, M.L. Trudeau, R. Schulz, J. Eletrochem. Soc. 140 (1993) 1974–1981.
[107] M.C.M. Alves, J.P. Dodelet, G. Guay, M. Ladouceur, G. Tourillon, J. Phys. Chem. 92 (1992) 10898–10905.
[108] M. Lefèvre, J.P. Dodelet, P. Bertrand, J. Phys. Chem. B 104 (2000) 11238–11247.
[109] M. Lefèvre, J.P. Dodelet, P. Bertrand, J. Phys. Chem. B 106 (2002) 8705–8713.
[110] M. Lefèvre, J.P. Dodelet, Electrochim. Acta 48 (2003) 2749–2760.
[111] M. Bron, J. Radnik, M.F. Erdmann, P. Bogdadoff, S. Fiechter, J. Electroanal. Chem. 535 (2002) 113–119.
[112] M. Lefèvre, J.P. Dodelet, P. Bertrand, J. Phys. Chem. B 109 (2005) 16718–16724.
[113] L. Liu, H. Kim, J.W. Lee, B.N. Popov, J. Electrochem. Soc. 154 (2007) A123–A128.
[114] Z.F. Ma, X.Y. Xie, X.X. Ma, D.Y. Zhang, Q. Ren, N.H. Mohr, V.M. Schmidt, Electrochem. Commun. 8 (2006) 389–394.
[115] G. Lalande, G. Faubert, R. Côté, D. Guay, J.P. Dodelet, L.T. Weng, P. Bertrand, J. Power Sources 61 (1996) 227–237.
[116] G. Faubert, R. Côté, D. Guay, J.P. Dodelet, G. Dénès, P. Bertrand, Electrochim. Acta 43 (1998) 345–353.
[117] S. Baraton, C. Coutanceau, C. Roux, F. Hahn, J.M. Léger, J. Electroanal. Chem. 577 (2005) 223–234.
[118] N. Alonso-Vante, H. Tributsch, Nature 323 (1986) 431–432.
[119] N. Alonso-Vante, W. Jaegermann, H. Tributsch, W. Hönle, K. Yvon, J. Am. Chem. Soc. 109 (1987) 3251–3257.
[120] N. Alonso-Vante, B. Schubert, H. Tributsch, A. Perrin, J. Catal. 112 (1988) 384–391.
[121] C. Fischer, N. Alonso-Vante, S. Fiechter, H. Tributsch, J. Appl. Electrochem. 25 (1995) 1004–1008.
[122] N. Alonso-Vante, in: W. Vielstich, A. Lamm, H.A. Gusteiger (Eds.), Handbook of Fuel Cells: Fundamentals, Technology and Applications. vol. 2. Electrocatalysis, Wiley, Chicester, 2003, pp. 534–543.

[123] R.W. Reeve, P.A. Christensen, A.J. Dicknson, A. Hamnett, K. Scott, Electrochim. Acta 45 (2000) 4237–4250.
[124] O. Solorz-Feria, K. Ellmer, M. Giersig, N. Alonso-Vante, Electrochim. Acta 39 (1994) 1647–1653.
[125] V.L. Rhun, N. Alonso-Vante, J. New. Mater. Electrochem. Syst. 3 (2000) 333–383.
[126] H. Tributsch, M. Bron, M. Hilgendorff, H. Schulenburg, I. Dorbandt, V. Eyert, P. Bogdanoff, S. Fiechter, J. Appl. Electrochem. 31 (2001) 739–748.
[127] F.J. Rodríguez, P.J. Sebastian, O. Solorza, R. Pérez, Int. J. Hydrogen Energy 23 (1998) 1031–1035.
[128] H. Cheng, W. Yuan, K. Scott, Electrochim. Acta 52 (2006) 466–473.